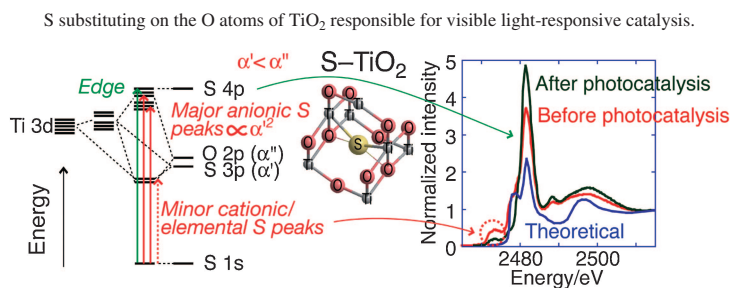# Monitoring of Sulfur Sites Doped in/on Titanium Oxide to Enable Photocatalysis under Visible Light Using S K-edge XANES

Yasuo Izumi[*1] and Yoshiyuki Shibata[2]

[1]*Department of Chemistry, Graduate School of Science, Chiba University,*
1-33 Yayoi, Inage-ku, Chiba 263-8522

[2]*Department of Nanomaterial Science, Graduate School of Advanced Integration Science, Chiba University,*
1-33 Yayoi, Inage-ku, Chiba 263-8522

S substituting on the O atoms of TiO_2 responsible for visible light-responsive catalysis.

Monitoring of Sulfur Sites Doped in/on Titanium Oxide to Enable Photocatalysis under Visible Light Using S K-edge XANES

Yasuo Izumi*[1] and Yoshiyuki Shibata[2]

[1]*Department of Chemistry, Graduate School of Science, Chiba University,*
1-33 Yayoi, Inage-ku, Chiba 263-8522
[2]*Department of Nanomaterial Science, Graduate School of Advanced Integration Science, Chiba University,*
1-33 Yayoi, Inage-ku, Chiba 263-8522

The electronic state and site structure of doped S to enable photocatalysis of TiO_2 under visible light were investigated using S K-edge XANES compared to theoretically generated spectra. S sites substituting on the O atoms of TiO_2 were predominant and essential in photocatalysis based on S K absorption edge peak energy and post-edge pattern. Minor cationic/ elemental S sites were detected as peaks due to the transition to vacant level of S3p, but most were lost during photocatalysis.

Photocatalysis has been investigated to decompose nitrogen oxides, sulfur oxides, and volatile organic compounds[1] and reduce water and carbon dioxide into hydrogen[2] and methanol/ formic acid,[3] respectively, over semiconductors, e.g., TiO_2. TiO_2 needs UV light to perform photocatalysis due to the band gap of 3.0–3.2 eV, but dopants effectively reduce the band gap to the visible light region.[4]

Electronic excitation from the valence band of TiO_2 to the impurity cationic V level and subsequent photoreduction over V–TiO_2 were monitored using V K-edge XAFS.[5–7] Charge recombination occurs less frequently in anion-doped TiO_2. Doped anions effectively reduce the band gap and promote photooxidation under visible light.[8] In this letter, the electronic structure of doped S sites in/on TiO_2 and the change during ethanol photooxidation were monitored using S K-edge XANES.

Two types of S-doped TiO_2 photocatalysts were prepared. One was synthesized by mixing thiourea with Ti tetraisopropoxide in a molar ratio of 1:2 during mesostructure formation using dodecylamine.[8] The S content in the sample after template removal and evacuation at 373 K was 1.7 wt %. The obtained catalysts were denoted SN-doped mesoporous TiO_2. Another was synthesized via CVD under 101 kPa of hydrogen sulfide with mesoporous TiO_2[8] separately synthesized using dodecylamine. The S contents in the samples were 0.48 and 0.77 wt % after CVD up to 583 and 623 K, respectively. Obtained catalysts were denoted as CVD-S-doped mesoporous TiO_2-583 or -623.

S K-edge XAFS spectra were measured at 290 K at the Photon Factory in High-Energy Accelerator Research Organization on beamline 9A (Proposal No. 2007G576). A Si(111) double crystal monochromator was fully tuned. Except for the S content evaluation in the sample based on the edge jump value in transmission mode, spectra were measured in fluorescence detection mode. A 1.4-mg portion of sample powder was ground as fine as possible and mounted on tape. The maximum of the first preedge feature in the spectrum of $Na_2S_2O_3 \cdot 5H_2O$ was assigned as 2472.02 eV.[9]

The S K-edge XANES spectra were theoretically generated using ab initio calculation code FEFF 8.4[10] operated in self-con-

sistent field and fully multiple scattering modes. The exchange-correlation potential of the Dirac–Hara and Hedin–Lundqvist imaginary part was chosen and corrected by adding a constant shift of -2.5 eV to the Fermi level. The energy of the theoretically generated spectrum was shifted by $+2.6$ eV to compare to the experimental data.

Twin peaks appeared at 2470.0 and 2471.9 eV for TiS_2 (Figure 1A-d). The energy difference between S3p and Ti3d is ca. 5 eV[11] and the energy levels interact in TiS_2 (Scheme 1a). The twin peaks were assigned to transition to $(1-\alpha^2)^{1/2}|Ti3d > -\alpha|S3p > (\equiv\Psi)$ levels. The intensity of this transition is proportional to the S3p character α^2 mixed into the wave function Ψ.[9,12]

Peak energies for S K post-edge spectrum for fresh SN-doped mesoporous TiO_2 (Figure 1A-a) were 2481.8(s), 2488.5(w),
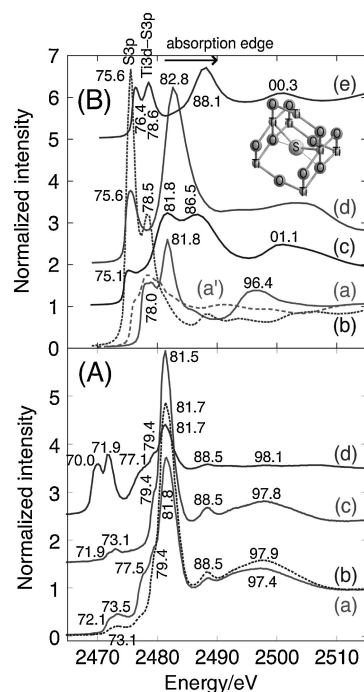

Figure 1. (A) Normalized S K-edge XANES spectra for SN-doped mesoporous TiO_2 before (a) and after ethanol oxidation under visible light (b), CVD-S-doped mesoporous TiO_2-623 after ethanol oxidation under visible light (c), and TiS_2 (d). (B) Theoretical S K-edge XANES spectra for S site substituting on the O atom (a) or Ti atom (b) of anatase-type TiO_2 or on the O atom at TiO_2(001) surface (a′), S site of SO_2 adsorbed on the Ti atom (c) or O atom (d) at TiO_2(001) surface, and S site of TiS_2 (e). (Inset) S substitution model on the O atom of TiO_2.
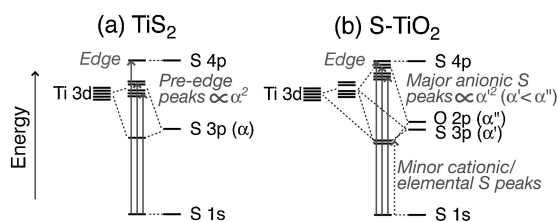
Scheme 1. Proposed energy diagram for TiS$_2$ (a) and S-doped mesoporous TiO$_2$ (b).

and 2497.4 eV(w,br) very similar to 2481.7, 2488.5, and 2498.1 eV for TiS$_2$ (Figure 1A-d). In contrast, the pre-edge feature was significantly suppressed at 2472.1 (sh) and 2473.5 eV for fresh SN-doped mesoporous TiO$_2$ compared to twin peaks for TiS$_2$. After catalysis in ethanol and O$_2$ gas under light $>$420 nm,[13] the pre-edge peak at 2473.1 eV and the shoulder peak at 2479.4 eV became even weaker (Figure 1A-b). The S K-edge XANES spectrum for CVD-S-doped mesoporous TiO$_2$ was essentially identical to that for SN-doped mesoporous TiO$_2$ both after photocatalysis (Figures 1A-b and 1A-c). Spectra for the former negligibly changed during photocatalysis.

We assumed anatase-type TiO$_2$[14,15] for theoretical calculations. Doped S substituted on O or Ti of the TiO$_2$ matrix (substitution model) or SO$_2$/SO$_3$H adsorbed on Ti or O at the TiO$_2$(001) surface.

The S K-edge XANES spectrum calculated for doped S model (total 261 atoms; Figure 1B, inset) substituting on the O of TiO$_2$ is depicted in Figure 1B-a. The S–Ti bond distance (R) was 2.283 Å (coordination number $N = 2$) based on Ti K-edge EXAFS for SN-doped mesoporous TiO$_2$.[8] The absorption edge peak at 2481.8 eV, shoulder peak(s) at 2478.0 eV, and broad post-edge peak at 2496.4 eV nicely reproduced Figure 1A-a. The post-edge pattern was somewhat similar to those of sulfates[16,17] probably because two O atoms were at 2.011 Å to doped S in the substitution model due to the strain of long Ti–S bonds in TiO$_2$ (Figure 1B, inset). When the $R_{S–Ti}$ was elongated to 2.44 Å (CVD-S-doped mesoporous TiO$_2$),[8] peaks in Figure 1B-a shifted within 1.2 eV toward lower energy but the spectral pattern was similar.

In the substitution model on Ti atom (no S site relaxation considered, total 261 atoms; Figure 1B-b) and SO$_2$ adsorption models on Ti ($R_{S–Ti} = 2.44$ Å, total 150 atoms; Figure 1B-c) or O atom ($R_{S–O} = 1.574$ Å, total 150 atoms; Figure 1B-d), the peaks at 2475.1–2475.6 eV became more intense as the S sites became more positive (Figure 1B-c → Figure 1B-d → Figure 1B-b). This peak was also observed for SO$_2$-adsorbed metal cluster.[9] Thus, weak pre-edge peaks appearing at 2471.9–2473.5 eV (Figures 1A-a–1A-c) were due to transition to S3p of minor cationic and/or elemental S sites[9] in S-doped mesoporous TiO$_2$ (Scheme 1b). The peaks at 2471.9–2473.5 eV became weaker after photocatalysis probably because cationic/elemental S species desorbed (Figures 1A-a and 1A-b).

Calculated spectra of adsorbed SO$_3$H either on Ti or O consisted of peaks at 2481.7 and 2504.0 eV, but the former peak was even broader than Figure 1B-d and did not match Figures 1A-a–1A-c. Intense peaks were reported to appear between 2482.4 and 2483.4 eV for Na, Mg, Al, K, Ca, Mn, Fe, and Ba sulfates[16,18] inconsistent with 2481.5–2481.8 eV for Figures 1A-a–1A-c. Because the catalysts could be used repeatedly for photocatalysis,[8] the substitutional S sites on the O atoms were concluded to be

photocatalytically active rather than cationic and/or elemental S sites.

The S sites substituting on the O atoms were not necessarily at the surface because the spectrum for S substituting on the O atom at the TiO$_2$(001) surface ($R_{S–Ti} = 2.283$ Å, $N = 2$, total 201 atoms; Figure 1B-a′) did not resemble any experimental spectra.

The twin pre-edge peaks and main peak in experimental data for TiS$_2$ (Figure 1A-d) were nicely reproduced at 2476.4, 2478.6, and 2488.1 eV in calculated Figure 1B-e.[19] However, the peaks shifted by 6.4–6.7 eV toward lower energy in the experiment. The reason for this discrepancy is not known, but limited model cluster size of TiS$_2$ (88 atoms) may be critical.

The twin peaks at 2470.0 and 2471.9 eV for TiS$_2$ due to transition to $(1 - \alpha^2)^{1/2}|\text{Ti3d} > -\alpha|\text{S3p} >$ (Scheme 1a) were not observed for S-doped TiO$_2$ mostly because latter Ti3d antibonding levels consist of greater O2p character than S3p (S contents in catalysts: 0.48–1.7 wt %). Smaller S3p character α'^2 in the antibonding levels led to the pre-edge peaks weaker. Additionally, the interaction between Ti3d and O2p and S3p may destabilize the antibonding levels more in S-doped TiO$_2$ near to S4p level (Scheme 1b) than in the case between Ti3d and S3p in TiS$_2$.

References
1 M. R. Hoffmann, S. T. Martin, W. Choi, D. W. Bahnemann, *Chem. Rev.* **1995**, *95*, 69.
2 A. Fujishima, K. Honda, *Nature* **1972**, *238*, 37.
3 V. Heleg, I. Willner, *J. Chem. Soc., Chem. Commun.* **1994**, 2113.
4 M. Anpo, *Bull. Chem. Soc. Jpn.* **2004**, *77*, 1427.
5 Y. Izumi, K. Konishi, H. Yoshitake, *Bull. Chem. Soc. Jpn.* **2008**, *81*, 1241.
6 Y. Izumi, K. Konishi, T. Miyajima, H. Yoshitake, *Mater. Lett.* **2008**, *62*, 861.
7 Y. Izumi, K. Konishi, D. M. Obaid, T. Miyajima, H. Yoshitake, *Anal. Chem.* **2007**, *79*, 6933.
8 Y. Izumi, T. Itoi, S. Peng, K. Oka, Y. Shibata, *J. Phys. Chem. C* **2009**, *113*, 6706.
9 Y. Izumi, T. Minato, K. Aika, A. Ishiguro, T. Nakajima, Y. Wakatsuki, in *Studies in Surface Science and Catalysis*, ed. by Gaigneaux, De Vos, Grange, Jacobs, Martens, Ruiz, Poncelet, Elsevier, Amsterdam, **2002**, Vol. 143A, pp. 361–368.
10 A. L. Ankudinov, B. Ravel, J. J. Rehr, S. D. Conradson, *Phys. Rev. B* **1998**, *58*, 7565.
11 G. Aschornack, *Handbook of X-ray Data*, Springer, Berlin/Heidelberg, **2007**.
12 A. Dey, Y. Jiang, P. O. de Montellano, K. O. Hodgson, B. Hedman, E. I. Solomon, *J. Am. Chem. Soc.* **2009**, *131*, 7869.
13 D. Masih, H. Yoshitake, Y. Izumi, *Appl. Catal., A* **2007**, *325*, 276.
14 D. T. Cromer, K. Herrington, *J. Am. Chem. Soc.* **1955**, *77*, 4708.
15 B. G. Hyde, S. Andersson, *Inorganic Crystal Structures*, John Wiley & Sons, New York, **1989**.
16 D. H. Kim, J. H. Kwak, J. Szanyi, S. J. Cho, C. H. F. Peden, *J. Phys. Chem. C* **2008**, *112*, 2981.
17 H. Dathe, A. Jentys, J. A. Lercher, *Phys. Chem. Chem. Phys.* **2005**, *7*, 1283.
18 J. Prietzel, J. Thieme, A. Herre, M. Salomé, D. Eichert, *Eur. J. Soil. Sci.* **2008**, *59*, 730.
19 Y. S. Kim, M. Mizuno, I. Tanaka, H. Adachi, *Jpn. J. Appl. Phys., Part 1* **1998**, *37*, 4878.